Journal of Alloys and Compounds 513 (2012) 55–60

Contents lists available at SciVerse ScienceDirect

Journal of Alloys and Compounds

journal homepage: www.elsevier.com/locate/jallcom

Suppressed phonon density and Para conductivity of Cd doped $Cu_{0.5}Tl_{0.5}Ba_2Ca_3Cu_{4-y}Cd_yO_{12-\delta}$ ($y = 0, 0.25, 0.5, 0.75$) superconductors

M. Rahim, Nawazish A. Khan*

Materials Science Laboratory, Department of Physics, Quaid-i-Azam University, Islamabad 4532, Pakistan

ARTICLE INFO

Article history:
Received 28 July 2011
Accepted 22 September 2011
Available online 10 October 2011

PACS:
74.70.−b
74.72.Jt
74.62.Bf

Keywords:
Fluctuation conductivity
Electron–phonon interactions
High temperature superconductors

ABSTRACT

The fluctuation-induced conductivity (FIC) above critical temperature (T_c) was measured in Cd doped $(Cu_{0.5}Tl_{0.5})Ba_2Ca_3(Cu_{4-y}Cd_y)O_{12-\delta}$ ($y = 0$, 0.25, 0.5, 0.75) as prepared and oxygen post-annealed superconductors using the Aslamazov–Larkin (AL) and Maki–Thompson (MT) models. From this FIC analysis the coherence length $\xi_{c(0)}$ along the c-axis, inter-plane coupling, dimensionality of fluctuations, the phase relaxation time τ_φ and Fermi velocity V_F of the carriers were calculated. All of the samples have shown 3D, 2D and 0D fluctuations above T_c. T^*, the temperature at which the resistivity curve deviates from the linear behavior, is shifted to lower temperatures with increasing Cd concentration. Width of the transition ΔT is shrunked with the enhanced Cd doping. The crossover temperature T_o is shifted to lower temperature values with increased Cd contents. Most likely these effects may be arising due to the replacement of Cu atoms by the heavier Cd atoms thereby producing inharmonic oscillations and causes suppression of the density of phonons which in turn suppress T^* and ΔT.

1. Introduction

The fluctuations induced conductivity (FIC) in oxide HTSC has always been observed due to their high anisotropy, short coherence length and low carrier densities. Thermal fluctuations well above the critical temperature (T_c) allow for a finite probability of the formation of the Cooper pairs which in turn induces excess conductivity $\Delta\sigma_{(T)}$ and therefore FIC plays a vital role to understand the microscopic properties of a material [1]. One of the reasons for the higher T_c in oxide HTSC is their excess conductivity resulting out of formation of the Cooper pairs well above the critical temperature. The formation of these Cooper pairs is local [2,3] and with decreasing the temperature, when $T = T_c$ of a compound, a steady state generation rate of cooper pairs dominates their decay rate. The additional conductivity $\Delta\sigma_{(T)}$ is explained by Aslamazov–Larkin (AL) equations [4] in thin films samples and by Lawrence–Doniach (LD) model in polycrystalline samples [5]. The AL equation is

$$\Delta\sigma_{AL} = A\varepsilon^{-\lambda D} \tag{1}$$

Here, λ_D is the dimensional exponent, $\lambda_D = 0.5$ and $A = \{e^2/[32\hbar\xi_{c(0)}]\}$ for 3D excess conductivity while $\lambda_D = 1.0$ and $A = \{e^2/[16\hbar d]\}$ for 2D excess conductivity, $e = (T - T_c^{mf})/T_c^{mf}$ is the reduced temperature, T_c^{mf} is the mean field critical temperature determined from the peak value of the temperature derivative of resistivity ($d\rho/dT$) in the transition region.

The expression for LD model is

$$\Delta\sigma_{LD} = \left[\frac{e^2}{16\hbar d}\right](1 + J\varepsilon^{-1})^{-1/2}\varepsilon^{-1} \tag{2}$$

where $J = [2\xi_{c(0)}/d]^2$ is a coupling parameter, $\xi_{c(0)}$ and d are the Ginzberg–Landau correlation length and the inter layer separation between the conducting layers respectively [6,7].

From Eq. (2), a cross-over from 3D to 2D is predicted at $\varepsilon = J$, and the corresponding cross-over temperature is denoted by T_o. The analysis of resistivity versus temperature data, confirms this cross-over. At this temperature the 2D and 3D competing conductivity processes of Cooper pairs meet. The system transforms from more isotropic three-dimensional (3D) conducting state to a two dimensional (2D) an-isotropic state with increasing the temperature. In oxide superconductors with conducting CuO_2 planes, the AL term dominates close to T_c. Since the formation of Cooper pairs takes place in the background of normal electrons, the effect of superconducting fluctuations on the conductivity of normal electrons is explained by Maki–Thompson (MT) term [8]. The MT part depends on the phase-relaxation time τ_φ and becomes significant in 2D fluctuations regime accompanied by moderate pair-breaking [6]. The Para conductivity is given by:

$$\Delta\sigma_{(T)} = \left[\frac{\rho_{N(T)} - \rho_{(T)}}{\rho_{N(T)}\rho_{(T)}}\right] \tag{3}$$

* Corresponding author. Tel.: +92 51 90642122; fax: +92 51 90642240.
E-mail address: nawazishalik2@yahoo.com (N.A. Khan).

0925-8388/$ – see front matter © 2011 Elsevier B.V. All rights reserved.
doi:10.1016/j.jallcom.2011.09.068

Table 1
The parameters extracted from the FIC analysis of $Cu_{0.5}Tl_{0.5}Ba_2Ca_3Cu_{4-y}Cd_yO_{12-\delta}$ ($y = 0, 0.25, 0.5, 0.75$) superconductors.

Sample	T_c (K)	T_0 (K) 3D–2D	T_0 (K) 2D–0D	T_c^{mf} (K)	T^* (K)	$\alpha = \rho_n$ (0 K) (Ω cm)	ΔT_c (K)	ξ_c (0) (Å)	$J = [2\xi_{c(0)}]^2/d^2$
As prepared									
$y = 0.0$	109.3	121.41	138.47	117.4	179.6	0.012	8.47	1.6504	0.03416
$y = 0.25$	107.3	120.41	139.48	114.3	175.5	0.002	7.39	2.04515	0.05263
$y = 0.5$	102	110.38	118.4	107.3	156.5	0.009	5.45	1.49016	0.02803
$y = 0.75$	81.28	106.36	135.46	102.35	174.65	0.359	2.68	1.76164	0.03918
Oxygen post-annealed									
$y = 0.0$	120.41	128.44	141.8	125.4	185	0.008	5.46	1.38336	0.024
$y = 0.25$	114.4	122.42	139.5	118.4	178	0.009	5.13	1.6427	0.03395
$y = 0.75$	81.28	110.38	124.43	105.36	148.28	0.673	3.92	1.94269	0.04765

Here, $\rho_{(T)}$ is the actually measured resistivity of the sample and $\rho_{N(T)} = \alpha + \beta T$ [$\rho_{N(T)} = 1/\sigma_{N(T)}$] is the extrapolated normal state resistivity to zero K; α is the intercept and β is the slope of straight line of $\rho_{N(T)}$. FIC analysis of the experimental data is a helpful tool to understand the intrinsic properties responsible for the mechanism of high temperature superconductivity. With the help of Para conductivity measurements one can find out the reliable values of $\xi_{c(T)}$, τ_φ, Fermi velocity of the carriers (V_F) and dimensionality of conductivity (D), etc. Since in oxide HTSC the carriers have very short Ginzburg–Landau correlation length $\xi_{GL(0)}$, it is advisable to carry out FIC analysis of temperature dependent conductivity $\Delta\sigma_{(T)} = \Delta\sigma_{RT}\varepsilon^{-\lambda D}$ well above T_c. The analysis is carried out via:

$$\ln\ \Delta\sigma_{(T)} = \ln \Delta\sigma_{RT} - \lambda_D \ln(\varepsilon) \tag{4}$$

Here, λ_D is the same as in Eq. (1) and has a value of 2.0 for 0D conductivity, zero dimension (0D) conductivity corresponds to the formation and breaking down of the Cooper pairs instantly with no preferred direction. The dimensionality and its exponent follow the relationship: $\lambda_D = 2D/2$ [9,10].

Excess conductivity analyses of $Bi_2Sr_2Ca_{n-1}Cu_nO_x$ ($n = 2, 3$) superconductors have shown 3D excess conductivity closer to the transition temperature whereas 2D conductivity regimes extended over much higher temperatures above T_c [11–14]. The excess conductivity analysis is done for thin films as well as for bulk samples of $YBa_2Cu_3O_{7-\delta}$ superconductors. In this case the polycrystalline bulk samples have shown 3D fluctuations in the neighborhood of transition region associated with a cross-over to 2D thermal fluctuations [7,10,15,16]. The thin films YBaCO samples have shown a mix of 2D to 3D regimes associated with a cross-over at a particular temperature T_o [16].

We have obtained enhanced superconducting properties by substitution of Zn ($3d^{10}$) at Cu ($3d^9$) planar sites in CuTl-1234 and CuTl-1223 superconductors with y up to 3.5 [17,18]. Cd ($4d^{10}$) is similar to Zn in electronic configuration and if there is no role of mass of the doping impurity on superconductivity, Cd should also have enhanced superconducting properties but contrary to this with the increasing substitution of Cd at Cu planar sites in $Cu_{0.5}Tl_{0.5}Ba_2Ca_3Cu_{4-y}Cd_yO_{12-\delta}$ ($y = 0, 0.25, 0.5, 0.75$) samples, the superconducting properties have been suppressed which are suggested to be arising due the inharmonic oscillations produced by the heavier Cd atoms in the CuO_2 planes resulting in the suppression of phonon population [19]. In this paper we present the FIC analyses of $Cu_{0.5}Tl_{0.5}Ba_2Ca_3Cu_{4-y}Cd_yO_{12-\delta}$ ($y = 0, 0.25, 0.5, 0.75$) samples to investigate the causes of suppression of T_c and the underlying mechanism of superconductivity.

2. Experimental

The samples were prepared by the usual solid state reaction method and were characterized by various techniques like dc-resistivity; ac-susceptibility, X-ray diffraction and Fourier transform infra-red spectroscopy (FTIR) measurements. The resistivity was measured by four-probe method and ac-susceptibility was measured with the help of a lock-in amplifier SR530. Bar shaped rectangular samples were used for ac-susceptibility and dc-resistivity measurements. During the resistivity measurement the contacts were made by silver paste and constant current of 1 mA was passed through the sample while the temperature was varied uniformly from 77 K to room temperature 290 K. Post-annealing of the samples was carried out in a tube furnace in Oxygen atmosphere at 550 °C for 5 h. The detailed method of preparation and characterization has already been reported elsewhere [19].

3. Results and discussion

We have followed the expression, $\Delta\sigma_{(T)} = \Delta\sigma_{RT}\varepsilon^{-\lambda D}$, for the fitting of resistivity versus temperature data for excess conductivity analyses in the neighborhood of transition region and above. The dimensional exponent values (λ_D) and a cross over temperature from the log plot of the excess conductivity versus the reduced temperature are mentioned in Tables 1 and 2. The λ_{3D} refers to the exponent value below T_o, the λ_{2D} to the value above T_o and λ_{0D} corresponds to exponent value of 2.0. The exponent λ_{0D} refers to the temperature point where Cooper pairs are formed and broken down instantly and their formation is not supported in any preferred direction. The values of λ_{3D}, λ_{2D} and λ_{0D} for as-prepared and oxygen post-annealed samples are given in Table 2. Due to predominant single phase nature of the samples we have assumed the small population of the defects in the CuO_2/CdO_2 planes. The cross-over temperature of 2D and 0D [from LD to Makki–Thompson (MT)] occurs at the point where, $\delta \simeq \alpha$, as in ref. [9] which gives:

$$\varepsilon_0 \simeq \frac{\pi\hbar}{1.203(l/\xi_{ab})(8k_BT\tau_\varphi)} \tag{5}$$

When the temperature of the sample is increased above T_c, at a particular point the mean free path l of the Cooper pair approaches ξ_{ab} and they are separated apart into Fermions. At this temperature (2D to 0D cross-over temperature T) the phase relaxation time of the Cooper-pair is estimated as:

$$\tau_\varphi = \frac{\pi\hbar}{8k_BT\varepsilon_0} \tag{6}$$

The FIC data is shown in the form of plots of $\ln(\Delta\sigma)$ versus $\ln\varepsilon$ for as-prepared $Cu_{0.5}Tl_{0.5}Ba_2Ca_3Cu_{4-y}Cd_yO_{12-\delta}$ ($y = 0, 0.25, 0.5, 0.75$) samples in Figs. 1–4 and for oxygen post-annealed samples in Figs. 5–7, respectively. The data of resistivity measurements versus temperature along with its derivative ($d\rho/dT$) is displayed in the inset of each figure; the derivative of the resistivity in the

Table 2
Dimensional exponents for 3D, 2D and 0D fluctuation regins of $Cu_{0.5}Tl_{0.5}Ba_2Ca_3Cu_{4-y}Cd_yO_{12-\delta}$ ($y = 0, 0.25, 0.5, 0.75$) samples.

$Cu_{0.5}Tl_{0.5}Ba_2Ca_3Cu_{4-y}Cd_yO_{12-\delta}$	λ_3	λ_2	λ_0
As prepared			
$y = 0.0$	−0.52	−0.95	−1.90
$y = 0.25$	−0.51	−0.95	−1.96
$y = 0.5$	−0.55	−0.98	−1.90
$y = 0.75$	−0.53	−1.12	−2.01
Oxygen post-annealed			
$y = 0.0$	−0.52	−0.92	−1.97
$y = 0.25$	−0.51	−0.95	−2.12
$y = 0.75$	−0.51	−1.11	−2.08

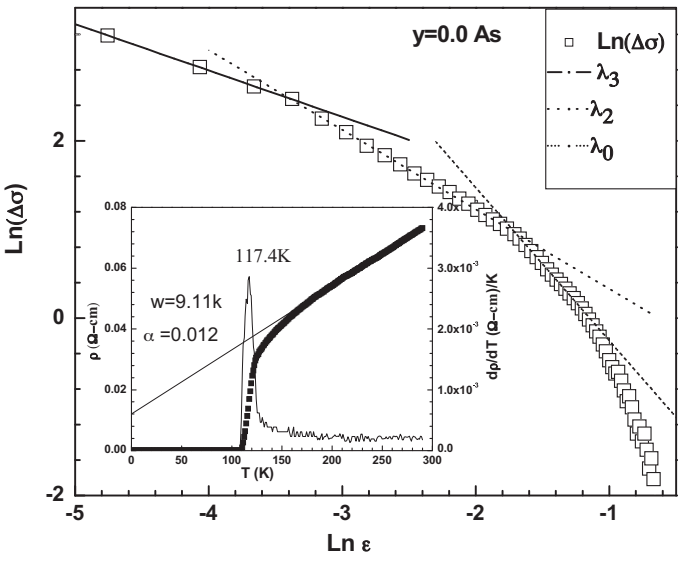

Fig. 1. $\ln(\Delta\sigma)$ versus $\ln(\varepsilon)$ plot of as prepared $Cu_{0.5}Tl_{0.5}Ba_2Ca_3Cu_{4-y}Cd_yO_{12-\delta}$ ($y = 0$) sample.

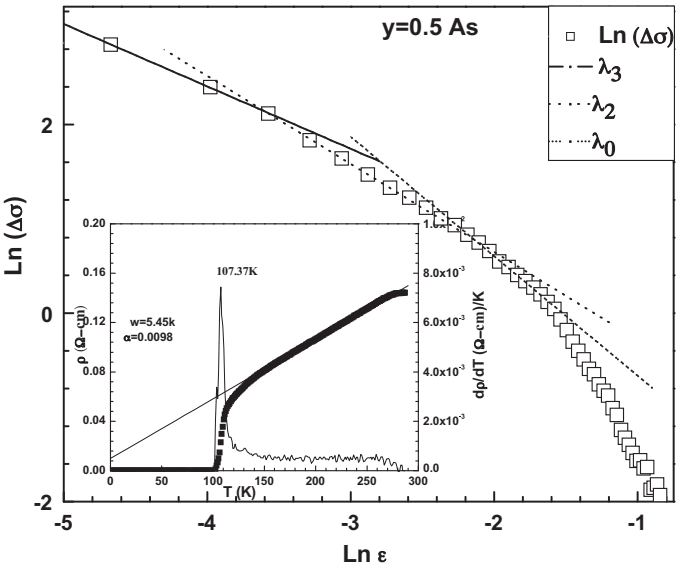

Fig. 3. $\ln(\Delta\sigma)$ versus $\ln(\varepsilon)$ plot of as prepared $Cu_{0.5}Tl_{0.5}Ba_2Ca_3Cu_{4-y}Cd_yO_{12-\delta}$ ($y = 0.5$) sample.

transition region has shown a single peak reminiscence of single phase nature of the material in each composition. The onset of excess conductivity starts at T^* (K), is found to be 179.6, 175.5, 156.5 and 174.65 K for as-prepared $Cu_{0.5}Tl_{0.5}Ba_2Ca_3Cu_{4-y}Cd_yO_{12-\delta}$ ($y = 0$, 0.25, 0.5, 0.75) samples respectively. Above T^* all the samples, i.e. ($y = 0$, 0.25, 0.5, 0.75) have shown linear dependence of resistivity versus temperature. At this temperature T^* (K) an onset of fluctuations in the order parameter of superconducting electrons sets in. T_o (K) is the temperature at which a cross over in the order parameter of the carriers from the 3D to 2D occurs. The as-prepared $Cu_{0.5}Tl_{0.5}Ba_2Ca_3Cu_{4-y}Cd_yO_{12-\delta}$ ($y = 0, 0.25$, 0.5, 0.75) samples have shown T_o (K) around 121.41, 120.41, 110.38 and 106.36 K respectively. The values of the parameters extracted from FIC analysis such as T_c, T_c^{mf}, α and the width of transition of various transition regimes (3D, 2D, etc.) are listed in Table 1 for as-prepared and oxygen post-annealed samples. The parameter α determines inter-grain connectivity and lower values are recommended for lower defects contribution to the residual resistivity of the samples. The α values determined for as-prepared $Cu_{0.5}Tl_{0.5}Ba_2Ca_3Cu_{4-y}Cd_yO_{12-\delta}$ ($y = 0$, 0.25, 0.5, 0.75) samples are 0.012, 0.002, 0.009, and 0.359 Ω cm, respectively. However, these values determined for oxygen post-annealed ($y = 0$, 0.25, 0.75) samples are 0.008, 0.009 and 0.673 Ω cm respectively. Except for higher Cd doping (i.e. $y = 0.75$), a lower values of α are observed in all Cd doped samples. The α values are not significantly altered for each concentration after post-annealing in oxygen which showed that small oxygen defects are present in the samples.

The contribution of FIC to 3D and 2D excess conductivities have been calculated by using the effective separation among the conducting CuO_2 planes "$d = 18$ Å" in this compound.

The λ_{3D} exponent values for as-prepared $Cu_{0.5}Tl_{0.5}Ba_2Ca_3Cu_{4-y}Cd_yO_{12-\delta}$ ($y = 0$, 0.25, 0.5, 0.75) samples are found to be around −0.52, −0.51, −0.55 and −0.53 in the temperature regimes 118.4–121.4, 115.4–120.41, 108.37–110.37 and 103.35–106.36 K, respectively; see Tables 2 and 3. This data showed 3D LD regime shifted to lower temperature values with the

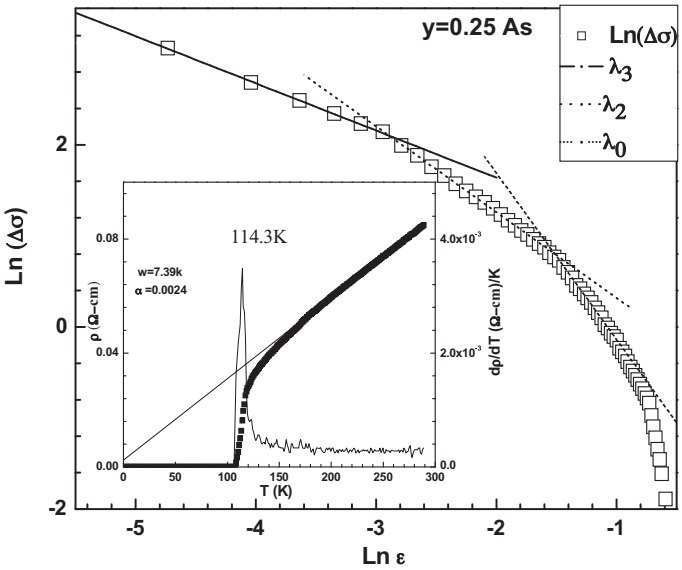

Fig. 2. $\ln(\Delta\sigma)$ versus $\ln(\varepsilon)$ plot of as prepared $Cu_{0.5}Tl_{0.5}Ba_2Ca_3Cu_{4-y}Cd_yO_{12-\delta}$ ($y = 0.25$) sample.

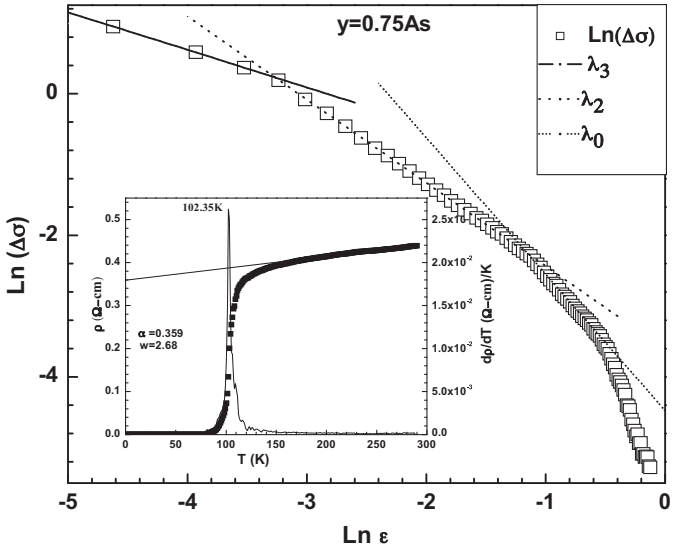

Fig. 4. $\ln(\Delta\sigma)$ versus $\ln(\varepsilon)$ plot of as prepared $Cu_{0.5}Tl_{0.5}Ba_2Ca_3Cu_{4-y}Cd_yO_{12-\delta}$ ($y = 0.75$) sample.

Table 3
Widths of 3D, 2D and 0D fluctuation regions observed from fitting of the experimental data of $Cu_{0.5}Tl_{0.5}Ba_2Ca_3Cu_{4-y}Cd_yO_{12-\delta}$ ($y = 0$, 0.25, 0.5, 0.75) samples using AL model.

$Cu_{0.5}Tl_{0.5}Ba_2Ca_3Cu_{4-y}Cd_yO_{12-\delta}$	λ_3 (temperature range) (K)	$\ln\varepsilon$ (range in 3D)	λ_2 (temperature range) (K)	$\ln\varepsilon$ (range in 2D)	λ_0 (temperature range) (K)	$\ln\varepsilon$ (range in 0D)
As prepared						
$y = 0.0$	118.4–121.41	−4.75 to −3.37	121.41–143.49	−3.37 to −1.5	143.49–154.53	−1.5 to −1.15
$y = 0.25$	115.4–120.41	−4.73 to −2.95	120.41–140.48	−2.95 to −1.51	140.48–160.55	−1.51 to −0.88
$y = 0.5$	108.37–110.38	−4.67 to −3.57	110.38–125.43	−3.57 to −1.78	125.43–131.45	−1.78 to −1.49
$y = 0.75$	103.35–106.36	−4.61 to −3.24	106.36–131.45	−3.24 to −1.25	131.45–165.57	−1.25 to −0.48
Oxygen post-annealed						
$y = 0.0$	126.4–128.44	−4.82 to −3.73	128.44–142.49	−3.73 to −2.05	142.49–159.55	−2.05 to −1.30
$y = 0.25$	119.4–122.42	−4.76 to −3.38	122.42–139.48	−3.38 to −1.72	139.48–158.54	−1.72 to −1.05
$y = 0.75$	106.36–110.38	−4.65 to −3.04	110.38–124.43	−3.04 to −1.70	124.43–129.44	−1.70 to −1.43

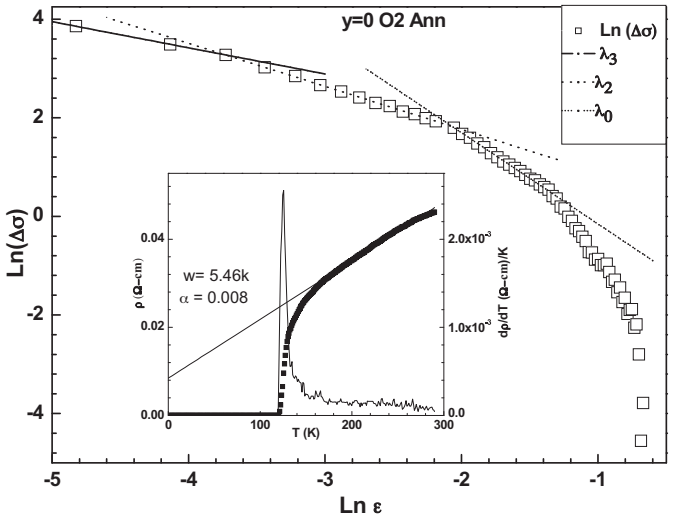

Fig. 5. $\ln(\Delta\sigma)$ versus $\ln(\varepsilon)$ plot of oxygen post-annealed $Cu_{0.5}Tl_{0.5}Ba_2Ca_3Cu_{4-y}Cd_yO_{12-\delta}$ ($y = 0$) sample.

increased Cd-doping. It is most likely that density of the phonon population is suppressed due to inharmonic oscillations produced by doped Cd atoms in the CuO_2/CdO_2 planes. The increased concentration of doped Cd atoms induce more and more suppression in phonon population consequently resulting into their decreased density essential for the electron–phonon interactions resulting into suppression of the critical regime and hence shift in the 3D LD regime to lower temperatures, Figs. 1–4. The 2D exponent above the cross-over temperature T_o for $Cu_{0.5}Tl_{0.5}Ba_2Ca_3Cu_{4-y}Cd_yO_{12-\delta}$ ($y = 0$, 0.25, 0.5, 0.75) as prepared samples are −0.95, −0.95, −0.98 and −1.12 in the temperature regimes 121.41–143.49, 120.41–140.48, 110.38–125.43 and 106.36–131.45 K, respectively. The λ_{0D} exponent beyond the termination of 2D regime for as prepared $Cu_{0.5}Tl_{0.5}Ba_2Ca_3Cu_{4-y}Cd_yO_{12-\delta}$ ($y = 0$, 0.25, 0.5, 0.75) samples are −1.90, −1.96, −1.90, −2.01 extended in the temperature regime 143.49–154.53, 140.48–160.55, 125.43–131.45 and 131.45–165.67 K respectively, see Tables 2 and 3.

Any possible role of concentration of mobile carriers in the conducting CuO_2/CdO_2 planes has been investigated by carrying out post-annealing of the samples in oxygen atmosphere; oxygen atoms through their higher electro-negativity can adjust the density of mobile carriers in the conducting planes. The $\ln(\Delta\sigma)$ versus $\ln(\varepsilon)$ plots of oxygen post-annealed $Cu_{0.5}Tl_{0.5}Ba_2Ca_3Cu_{4-y}Cd_yO_{12-\delta}$ ($y = 0$, 0.25, 0.75) samples are shown in Figs. 5–7, respectively. The values of dimensional exponents for 3D AL and 2D AL regions, determined from these plots are given in Table 2 and their corresponding widths are given in Table 3. The λ_{3D} exponent values for oxygen post-annealed $Cu_{0.5}Tl_{0.5}Ba_2Ca_3Cu_{4-y}Cd_yO_{12-\delta}$ ($y = 0$, 0.25, 0.75) samples are −0.52, −0.51 and −0.51 in the temperature regimes 126.46–128.44, 119.40–122.42 and 106.36–110.38 K, respectively, see Tables 2 and 3. This data showed that in comparison with as-prepared samples the 3D AL regime shifted to higher temperatures in all $Cu_{0.5}Tl_{0.5}Ba_2Ca_3Cu_{4-y}Cd_yO_{12-\delta}$ ($y = 0$, 0.25, 0.75) samples. These experiments provided an unequivocal evidence of role of enhance density of the electrons in the conducting CuO_2/CdO_2 planes and hence increased electron–phonon interactions consequently pushing the set in regime of 3D AL towards higher

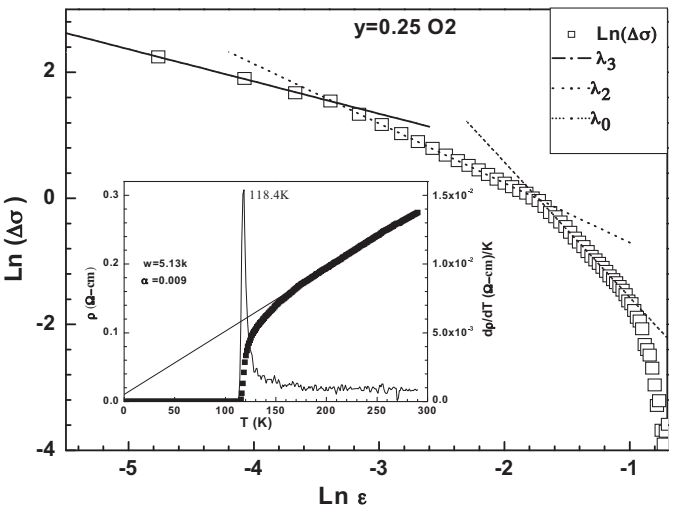

Fig. 6. $\ln(\Delta\sigma)$ versus $\ln(\varepsilon)$ plot of oxygen post-annealed $Cu_{0.5}Tl_{0.5}Ba_2Ca_3Cu_{4-y}Cd_yO_{12-\delta}$ ($y = 0.25$) sample.

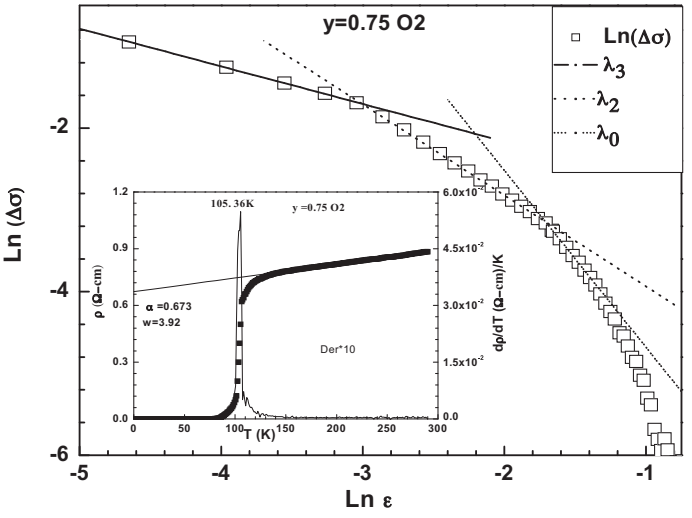

Fig. 7. $\ln(\Delta\sigma)$ versus $\ln(\varepsilon)$ plot of oxygen post-annealed $Cu_{0.5}Tl_{0.5}Ba_2Ca_3Cu_{4-y}Cd_yO_{12-\delta}$ ($y = 0.75$) sample.

Table 4
Fermi velocity V_F, phase-relaxation time for cooper pair τ_φ, coupling constant λ, and energy E required to break apart the Cooper pair of $Cu_{0.5}Tl_{0.5}Ba_2Ca_3Cu_{4-y}Cd_yO_{12-\delta}$ ($y = 0$, 0.25, 0.5, 0.75) samples.

Sample	$V_F = \frac{5\pi k_B T_c \xi_{c(0)}}{2K\hbar}$ ($\times 10^7$ cm/s)	$\tau_\varphi = \frac{\pi\hbar}{8k_B T\varepsilon_0}$ (10^{-13} s)	$\lambda = \frac{\hbar\tau_\varphi^{-1}}{2\pi k_B T}$	$E = \frac{h}{\tau_\varphi(1.6\times10^{-19})}$ (eV)
As prepared				
$y = 0.0$	1.546	0.945647	0.08962	0.044
$y = 0.25$	1.881	0.941221	0.09197	0.044
$y = 0.5$	1.306	1.42931	0.06783	0.030
$y = 0.75$	1.226	0.806896	0.11465	0.051
Oxygen annealed				
$y = 0.0$	1.427	1.55612	0.05484	0.027
$y = 0.25$	1.609	1.21444	0.07179	0.034
$y = 0.75$	1.352	1.33922	0.07297	0.031

temperatures; Figs. 5–7. The 2D AL regime in comparison with as-prepared samples is shifted towards higher temperatures in oxygen post-annealed $Cu_{0.5}Tl_{0.5}Ba_2Ca_3Cu_{4-y}Cd_yO_{12-\delta}$ ($y = 0$, 0.25, 0.75) samples. The λ_{2D} exponent values above the cross over temperature T_o for $Cu_{0.5}Tl_{0.5}Ba_2Ca_3Cu_{4-y}Cd_yO_{12-\delta}$ ($y = 0$, 0.25, 0.75) Oxygen post-annealed samples are −0.92, −0.95 and −1.11 in the temperature regimes 128.44–142.49, 122.42–139.48 and 110.38–124.43 K respectively, Tables 2 and 3. The shift in 2D AL regime to higher temperature also compliments the role of enhanced density of carriers in CuO_2/CdO_2 planes in the increased electron–phonon interactions. However, in oxygen post-annealed $Cu_{0.5}Tl_{0.5}Ba_2Ca_3Cu_{4-y}Cd_yO_{12-\delta}$ ($y = 0$, 0.25, 0.75) samples a small suppression in the termination end of 2D AL regimes or setting in of 0D AL regime in comparison with as-prepared samples is observed. This suppression is most likely originating from the optimization of density of carriers in the conducting CuO_2/CdO_2 planes. The λ_{0D} exponent beyond the termination of 2D regime are −1.97, −2.12, −2.08 and are extended in the temperature regimes 142.49–159.55, 139.48–1158.54 and 124.43–129.44 K for Oxygen post-annealed samples $Cu_{0.5}Tl_{0.5}Ba_2Ca_3Cu_{4-y}Cd_yO_{12-\delta}$ ($y = 0$, 0.25, 0.75) respectively, see Tables 2 and 3.

In order to find out the coherence length $\xi_{c(0)}$ along c-axis and the inter-layer coupling constant $J = [4\xi_{c(0)}]^2/d^2$ we have used the expressions of Lawrence–Doniach (LD) model for cross-over temperature $T_o = T_c[1 + (2\xi_{c(0)}/d)^2]$, where d is the inter-layer distance between CuO_2/CdO_2 planes, and in the present case $d = 18$ Å, is used for the calculations of these parameters of our $Cu_{0.5}Tl_{0.5}Ba_2Ca_3Cu_{4-y}Cd_yO_{12-\delta}$ ($y = 0$, 0.25, 0.5, 0.75) samples [20]. The coherence length $\xi_{c(0)}$ along the c-axis for as-prepared and oxygen post-annealed samples are given in Table 1. For $Cu_{0.5}Tl_{0.5}Ba_2Ca_3Cu_{4-y}Cd_yO_{12-\delta}$ ($y = 0$, 0.25, 0.5, 0.75) as-prepared samples the $\xi_{c(0)}$ values are 1.6504, 2.045, 1.49, 1.76 Å and J values are 0.034, 0.052, 0.028, 0.0391 respectively (Table 1). Whereas, for oxygen post-annealed $Cu_{0.5}Tl_{0.5}Ba_2Ca_3Cu_{4-y}Cd_yO_{12-\delta}$ ($y = 0$, 0.25, 0.75) samples the values of $\xi_{c(0)}$ are observed to be 1.383, 1.642 and 1.942 Å and the values of J are 0.024, 0.0339 and 0.047 respectively (Table 1). Since the coherence length along the c-axis critically depends on the density of the carriers [$K_F = (3\pi^2 N/V)^{1/3}$ and $\xi_c = \hbar K_F/2m\Delta$ where K_F is Fermi-vector] in the conducting CuO_2/CdO_2 planes, the values of which are not significantly altered with the incorporation of Cd showing that suppression of 3D AL and 2D LD regimes is intrinsically arising from the suppression in the density of phonons. The values of inter-layer coupling also compliment this conjecture, since the values of J parameter is not significantly altered.

A cross-over of LD–MT transition predicted in HL theory [6] is also witnessed in the log plot of the data of excess conductivity versus the reduced temperature. From the cross over of λ_{2D} and λ_{0D} (LD to MT transition) the phase relaxation time τ_φ of the Cooper pair is determined. By using this phase relaxation time the coupling constant $\lambda = \hbar\tau_\varphi^{-1}/2\pi k_B T$, the Fermi velocity of the carriers $V_F = 5\pi k_B T_c \xi_{c(0)}/2K\hbar$ ($K \cong 0.12$ is a co-efficient of proportionality as used in Ref. [2]), and the energy required to break apart the Cooper pairs $E = h/\tau_\varphi(1.6 \times 10^{-19})$ (eV) are determined [15,21], see Table 4. The values of τ_φ are in the range of 10^{-13} s which are comparable to the values found in other oxide superconductors. Since the coupling constant λ values are greater than 0.04 showing the priority mechanism of superconductivity to be electron–phonon interaction; the electron–electron correlation effect is minimum [21]. Since the values of V_F, τ_φ, λ and E as given in Table 4, are not significantly altered in $Cu_{0.5}Tl_{0.5}Ba_2Ca_3Cu_{4-y}Cd_yO_{12-\delta}$ ($y = 0$, 0.25, 0.5, 0.75) samples, this also compliment and supports our belief that the suppression in the 3D AL and 2D LD regimes is arising from the decreased density of phonon population arising due to Cd-doping in the final compound.

4. Conclusions

$Cu_{0.5}Tl_{0.5}Ba_2Ca_3Cu_{4-y}Cd_yO_{12-\delta}$ ($y = 0$, 0.25, 0.5, 0.75) samples are successfully synthesized at 880 °C and their superconducting properties have been studied. The zero resistivity critical temperature is decreased with the increasing Cd-doping in the final compound. The FIC analysis carried out by employing LD model in the mean field region, have shown that 3D LD regime along with the cross over temperature T_o shifted to lower temperatures with increased doping of Cd. Since the $\xi_c(0)$, J, V_F, τ_φ, λ and E are not significantly modified with increased Cd-doping, the suppression in the 3D AL/LD regime and hence the $T_c(R = 0)$ lead us to a conclusion that density of the phonon population is suppressed due to inharmonic oscillations produced by doped Cd atoms in the CuO_2/CdO_2 planes which ultimately results in decreased superconducting properties. The systematic suppression of critical regime and hence the $T_c(R = 0)$ to lower temperatures with increased Cd concentration also supports this conclusion.

Acknowledgements

Higher Education Commission of Pakistan (HEC) through project No. 20-1482/R&D/09-1472 and Internal Center for Theoretical Physics (ICTP) through project number PRJ-27 are acknowledged for their financial supports.

References

[1] U.C. Upreti, A.V. Narlikar, Solid State Commun. 100 (1996) 615–620.
[2] A.L. Solovjov, V.M. Dmitriev, Low Temp. Phys. 35 (2009) 169.
[3] A.L. Solovjov, V.M. Dmitriev, Low Temp. Phys. 32 (2006) 99.
[4] L.G. Aslamazov, A.L. Larkin, Phys. Lett. A 26 (1968) 238.
[5] W.E. Lawrence, S. Doniach, in: E. Kanda (Ed.), Proceedings of the Twelfth International Conference on Low Temperature Physics, Keigaku, Tokyo, 1971, p. 361.
[6] S. Hikami, A.I. Larkin, Mod. Phys. Lett. B 2 (1988) 693;
Also in: B. Oh, K. Char, A.D. Kent, M. Naito, M.R. Beasley, T.H. Geballe, R.H. Hammond, A. Kapitulnik, J.M. Grabeal, Phys. Rev. B 37 (1988) 7861.
[7] A.K. Ghosh, S.K. Bandyopadhyay, P. Barat, P. Sen, A.N. Basu, Physica C 264 (1996) 255.
[8] K. Maki, Prog. Theor. Phys. 39 (1968) 897;
R.S. Thompson, Phys. Rev. B 1 (1970) 327.

[9] A.L. Solovjov, H.-U. Habermeier, T. Haage, Fiz Nizk. Temp. 28 (2002) 24 [Low Temp. Phys. 28 (2002) 17].
[10] T. Sato, H. Nakane, S. Yamazaki, N. Mori, S. Hirano, S. Yoshizawa, T. Yamaguchi, Physica C 392–396 (2003) 643–647.
[11] M.-O. Mun, S.-I. Lee, S.-H.S. Salk, H.J. Shin, M.K. Joo, Phys. Rev. B 48 (1993) 6703.
[12] N. Mori, J.A. Wilson, H. Ozaki, Phys. Rev. B 45 (1992) 10633.
[13] S.H. Han, O. Rapp, Solid State Commun. 94 (1995) 661.
[14] A.K. Ghosh, A.N. Basu, Phys. Rev. B 59 (1999) 11193–11196.
[15] A.L. Solovjov, H.-U. Habermeier, T. Haage, Fiz Nizk. Temp. 28 (2002) 144 [Low Temp. Phys. 28 (2002) 99].
[16] M. Kaur, R. Srinibasan, G.K. Mehta, D. Kanjilal, R. Pinto, S.B. Ogale, S. Mohan, V. Ganesan, Physica C 443 (2006) 61.
[17] N.A. Khan, M. Mumtaz, Supercond. Sci. Technol. 19 (2006) 762–766.
[18] N.A. Khan, M. Mumtaz, J. Low Temp. Phys. 149 (2007) 97–103.
[19] N.A. Khan, M. Rahim, J. Alloys Compd. 481 (2009) 81–86.
[20] J.L. Tallon, J.R. Cooper, P.S.I.P.N. de Silva, G.V.M. Willians, J.W. Loram, Phys. Rev. Lett. 75 (1995) 4114.
[21] A.L. Solovjov, V.M. Dmitriev, H.-U. Habermeier, Phys. Rev. B 55 (1997) 8551.